MOLEKUL
eISSN: 2503-0310

Articles
https://doi.org/10.20884/1.jm.2026.21.2.19280

Structural Characterization and Antidiabetic Drug Potential of Aminated Eugenol Derivatives Synthesized via Ultrasound-Assisted Method

Riska Mardiyanti[1]*, Jumina[2], Nunuk Hariani Soekamto[1], Nur Umriani Permatasari[1], Bulkis Musa[1], Muhammad Al Mustawa[1]

[1]Department of Chemistry, Faculty of Mathematics and Natural Sciences, Hasanuddin University, Kampus Unhas Tamalanrea, Makassar, 90245, Indonesia.
[2]Department of Chemistry, Faculty of Mathematics and Natural Sciences, Gadjah Mada University, Sleman, Yogyakarta, 55281, Indonesia.

*Corresponding author email: riskamardiyanti@unhas.ac.id

Received January 14, 2026; **Accepted** May 31, 2026; **Available online** July 20, 2026

ABSTRACT. Diabetes mellitus remains a global health challenge, necessitating the development of more effective α-amylase inhibitors with fewer side effects than current synthetic drugs. This study reports the successful synthesis of three aminated eugenol derivatives, **a** (1-(4-allyl-2-methoxyphenoxy)-3-(phenylamino)propan-2-ol), **b** (1-(4-allyl-2-methoxyphenoxy)-3-(m-tolylamino)propan-2-ol), and **c** (1-(4-allyl-2-methoxyphenoxy)-3-((4 chlorophenyl)amino)propan-2-ol), via ultrasonically assisted epoxide ring-opening using aniline, m-toluidine, and 4-chloroaniline. Ultrasonic irradiation significantly reduced the reaction time from 5-24 hours to 2 hours. Structural characterization by FTIR, ^{1}H-NMR, ^{13}C-NMR, GC-MS, and melting point analysis confirmed the successful formation of all derivatives. In vitro α-amylase inhibition assays (UV–Vis) showed that all compounds exhibited higher inhibitory activity than acarbose, with compound b demonstrating the strongest inhibition (99.04% at 250 μM). Molecular docking studies against α-amylase (PDB: 1B2Y) further supported these results, yielding binding energies of –4.58, –5.13, and –5.16 kcal mol^{-1} for compounds **a**, **b**, and **c**, respectively, compared with –3.64 kcal mol^{-1} for acarbose. These findings demonstrate the enhanced efficiency of the ultrasound-assisted synthesis and substituent variations enhance both the structural and biological properties of the eugenol derivatives, offering critical perspectives on how their molecular structure dictates activity, thereby validating their future utility as promising antidiabetic drug candidates.

Keywords: α-amylase binding affinity, epoxide ring-opening, sonochemical synthesis, structure-activity relationship, substituent electronic effect.

INTRODUCTION

Diabetes mellitus remains a global metabolic challenge characterized by elevated blood glucose levels, primarily classified into Type I and Type II (Roy et al., 2024). Type I diabetes involves the autoimmune destruction of pancreatic β-cells, while Type II accounts for approximately 90% of global cases and arises from insulin resistance (Fatiha et al., 2018; Cerna, 2020). Current therapeutic strategies, such as the use of acarbose and metformin, are often limited by significant gastrointestinal side effects (Nampoothiri et al., 2011). Although herbal medicines offer a more natural alternative, they frequently face issues regarding compound instability (Chaudhari et al., 2023). Consequently, there is an urgent need to develop new, stable, and more effective α-amylase inhibitors with minimized side effects.

Eugenol, a major phenolic compound found in clove (*Syzygium aromaticum*), is a versatile building block for synthesizing secondary metabolites like 6-gingerol, cimiracemate B, and obovatol (Kaufman, 2015; Molina-Gutiérrez et al., 2019). Its unique structure, featuring conjugated aromatic and allyl systems, allows for diverse electronic modifications that influence molecular interactions with enzyme active sites (Guan et al., 2023; Julianto et al., 2023). While *in* vivo studies show eugenol can reduce α-amylase activity and lower blood glucose by up to 60% (Mnafgui et al., 2013), previous syntheses of aminated eugenol derivatives using conventional heating required 24 hours and focused primarily on α-glucosidase inhibition (Bilgiçli et al., 2019). Consequently, the detailed correlation between specific nitrogen-based substituents and their binding behavior toward α-amylase remains poorly understood, leaving a significant gap in the systematic understanding of their structure-activity relationships (SARs) and more efficient synthetic routes.

Given the substantial potential of eugenol derivatives, particularly those containing the

aminopropoxy moiety for α-amylase inhibition and related antidiabetic mechanisms (Julianto et al., 2023), systematic structural studies on these systems are highly relevant. However, the synthesis of these derivatives presents a significant technical challenge, as conventional methods typically rely on reflux or heating for up to 24 hours (Nasef et al., 2016; Bilgiçli, 2019). While ultrasound-assisted organic synthesis has emerged as a sustainable green alternative to accelerate reaction kinetics (Ziarani et al., 2019; Shabalala et al., 2020), its application for the amination of eugenol remains unreported. To address these gaps, this study establishes a rapid, ultrasound-assisted route for synthesizing aminated eugenol derivatives. The inhibitory activity of the synthesized compounds against α-amylase was evaluated through in vitro assays using UV-Vis spectrophotometry. By combining these experimental results with comprehensive spectroscopic characterization (FTIR, NMR, GC-MS), in vitro study and molecular docking simulations, this research aims to elucidate how specific electronic substituents modulate α-amylase interaction, providing critical insights for the development of future antidiabetic candidates.

EXPERIMENTAL SECTION

Chemicals and Reagents

The chemicals enrolled in this research consisted of eugenol 99% (Dynasti Group), epichlorohydrin (Sigma-Aldrich), ethyl acetate (Merck), sodium hydroxide (NaOH; Smart Lab), magnesium sulfate ($MgSO_4$; Merck), potassium carbonate (K_2CO_3; Sigma-Aldrich), n-hexane (Smart Lab), chloroform (Merck), diethyl ether (Sigma-Aldrich), methanol (Merck), and the amine reagents aniline, m-toluidine, and 4-chloroaniline (Sigma-Aldrich). Column chromatography silica gel (60 G, Merck), TLC silica plates (Merck), Whatman No. 42 filter paper, and distilled water. For the preliminary α-amylase inhibition assays, the materials included α-amylase enzyme (Xi'an Lyphar Biotech Co., Ltd), soluble starch (Merck), iodine solution 0.2% (Brataco), HCl 1% (Smart Lab), acarbose (Sigma-Aldrich), and phosphate buffer pH 6.9 (Merck).

Materials

Synthetic and analytical experiments utilized standard laboratory glassware, a reflux apparatus, and an ultrasonic cleaner (EHRET Typ. BK 3108, 50 Hz, 200 W). Analytical instruments included FTIR spectrophotometer (Shimadzu Prestige-21), GC–MS and DI–MS (Shimadzu QP2010S), LC–MS (Xevo G2-S QTof), melting point Apparatus, and NMR spectrometer (JEOL JNM-ECZ 500 MHz). For the α-amylase assay and absorbance measurements, a UV–Visible spectrophotometer (Shimadzu UV-1800) was used.

Synthesis Procedure

Synthesis of Precursor Compound

Following the reported procedure (Bilgiçli, 2019), sodium hydroxide (0.24 g, 6.6 mmol) was dissolved in 10 mL distilled water and added dropwise to a mixture of eugenol (1.084 g, 6.6 mmol) and epichlorohydrin (10 mL) at 85 °C under vigorous stirring for 30 min. The resulting mixture was partitioned with ethyl acetate (20 mL). The organic layer was then washed with brine (2 × 15 mL), dried using anhydrous $MgSO_4$, and evaporated under vacuum to afford the oxirane intermediate 2-((4-allyl-2-methoxyphenoxy)methyl) oxirane. The precursor was purified and characterized by FTIR, and GC–MS analyses.

Ultrasound-Assisted Synthesis of Eugenol Derivatives

The synthesis was conducted by adapting the chemical procedure from Bilgiçli et al. (2019) with a sonochemical (50 Hz, 200 Watt) (Nasef et al., 2016). The oxirane precursor (1 mmol) was mixed with saturated K_2CO_3 (2 mL) and an amine compound (3 mmol) at room temperature under ultrasonic irradiation for 2 h. The disappearance of starting material was tracked using TLC. Post-reaction, the mixture was extracted into ethyl acetate, washed with water, and cleared of residual moisture with anhydrous $MgSO_4$. Solvent evaporation yielded a residue that was refined first by recrystallization from a mixture of diethyl ether and n-hexane, and then by chromatographic separation to ensure high purity. The products were obtained as compounds **a**, **b**, and **c** in yields of 91.66, 89.34, and 97.24%, respectively. Structural confirmation was conducted by FTIR, ^{1}H-NMR, ^{13}C-NMR, and MS analyses, verifying the successful ring-opening of the oxirane and formation of aminopropoxy linkages. The synthetic pathway is illustrated in **Figure 1**.

Preliminary Enzyme–Ligand Interaction Study (In Vitro Assay)

To examine the interaction tendencies of the synthesized derivatives toward α-amylase, a modified starch–iodine colorimetric method was adopted following previously reported protocols (Rafique et al., 2020; Ahmed et al., 2023). A 10 mL starch substrate was treated with 1 mL of the sample (62.5–1000 μM) and 0.5 mL of the enzyme solution. The reaction environment was regulated at 37 °C for a duration of 10 min to allow for enzymatic activity. After incubation, the reaction was quenched via the sequential introduction of 1 mL of 1% HCl and 0.1 mL of 0.2% iodine. Subsequently, the optical density was recorded at a wavelength of 540 nm, with the degree of inhibition determined in accordance with Equation (1) derived from the original study to compare the relative interaction capability of each compound. These results served as qualitative indicators supporting the structure–interaction discussion, rather than quantitative bioactivity tests. The detailed composition of each system is presented in **Table 1.**

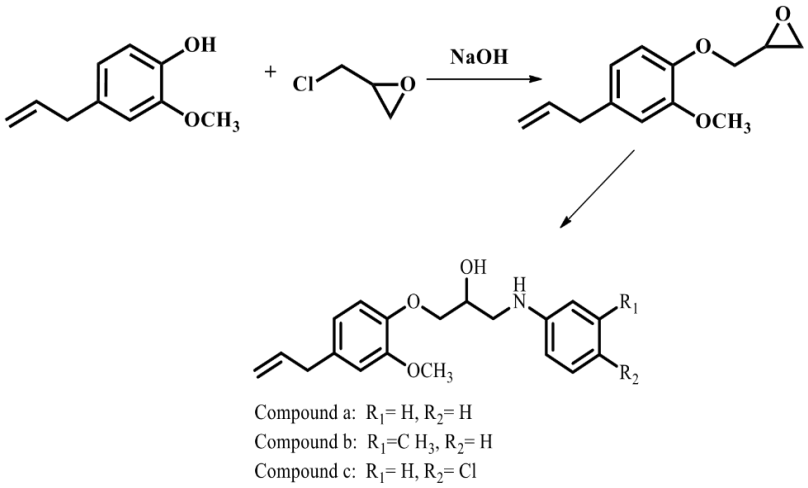

Figure 1. Synthetic pathway compound a, b, and c.

Table 1. Composition of reactants in the system

Type of solution	Blank (mL)	Control (mL)	S_0 (mL)	S_1 (mL)
Sample	-	-	1	1
Substrate	10	10	10	10
Enzyme	-	0.5	-	0.5
	Incubation at 37 °C for 10 minutes			
HCl 1%	-	1	-	1
Iodine 0,2%	0.1	0.1	0.1	0.1

The absorbance obtained is then calculated using Equation 1 as follows:

$$\% \text{ Inhibition} = \frac{(A_{\text{blank}}-A_{\text{control}})-(A_{S0}-A_{S1})}{(A_{\text{blank}}-A_{\text{control}})} \quad (1)$$

Description:
A_{S1} = Absorbance of systems containing substrates, enzymes and samples
A_{S0} = Absorbance of systems containing substrates, samples without enzymes
$A_{control}$ = Absorbance of systems containing substrates, enzymes without samples
A_{blank} = Absorbance of systems containing substrates without enzymes and samples

Molecular Interaction Analysis (In Silico Docking Study)

In silico interrogations were conducted via the AutoDock **Tools 1.5.7** suite. To anticipate preferred binding orientations and thermodynamic stability, each ligand was simulated within the catalytic pocket of alpha-amylase (PDB entry: 1b2y). The search space was confined to a cubic grid (40 x 40 x 40 Å) with a fine resolution of 0.375 Å, with all configurational settings archived in gpf format. The docking process was configured to produce 10 conformations using the Lamarckian Genetic Algorithm (LGA) to calculate binding energies and predict inhibition constants. Validation of the docking protocol was carried out by re-docking the standard ligand at the enzyme's active site, with an acceptable RMSD ≤ 2 Å (Saputri et al., 2016; Wang et al., 2024). The resulting docking poses and interaction profiles were visualized and analyzed using Discovery Studio Visualizer (Patel et al., 2023).

RESULTS AND DISCUSSION

The aminated derivatives of eugenol were successfully synthesized via ultrasound-assisted ring opening of the oxirane intermediate with different amine compounds (aniline, m-toluidine, and 4-chloroaniline). Ultrasound irradiation markedly accelerated the reaction, reducing the time from the conventional 5–24 h to only about 2 h while maintaining high yields compound **a** (91.66%), **b** (89.34%), and **c** (97.24%). This improvement in both rate and yield aligns with previous findings demonstrating the catalytic role of ultrasound in accelerating organic transformations (Bilgiçli et al., 2020). Ultrasonic cavitation enhances mass transfer and molecular collisions, thereby increasing reaction efficiency and purity. Similar studies have reported 5–20-fold faster reaction rates and high yields (95–99%) in multicomponent or solvent-assisted systems, validating ultrasound as an effective green method for promoting chemical transformations (Thirumalaikumar, 2022; Ekbrant et al., 2021). Although several investigations on eugenol derivatives have been reported (Bilgiçli et al., 2016; Bilgiçli et al., 2020), none have employed ultrasound irradiation as the primary synthetic method. In this study, reaction time was successfully reduced from the conventional 5–24 h to only 2 h, consistent with

previous observations of ultrasonic acceleration in organic reactions.

Mechanism of Reactions:

Synthesis of precursor compound 2-((4-allyl-2-methoxyphenoxy)methyl)oxirane

The reaction between eugenol and epichlorohydrin to form the epoxide-substituted eugenol proceeds through a nucleophilic substitution mechanism under basic conditions. The detailed reaction mechanism for the formation of the epoxide-substituted eugenol is presented in **Figure 2**.

Reaction mechanism for the formation of the aminated eugenol derivatives a, b, and c

Formation eugenol derivatives a, b and c occurred via nucleophilic ring-opening of the oxirane intermediate by the amine's lone pair, forming a new C–N bond and a β-hydroxyl group. This mechanism agrees with established amine-mediated epoxide opening processes described in previous studies (Thirumalaikumar, 2022; Ekbrant et al., 2021). This reactions mechanism can be seen in **Figure 3**.

The reaction time was significantly reduced from 24 to 2 hours due to ultrasonic irradiation (50 Hz, 200 W), which induces acoustic cavitation. According to Ling et al. (2018), the violent collapse of cavitation bubbles generates mechanical micro jets and shock waves that enhance mass transfer and overcome steric hindrance through effective molecular collisions. Furthermore, these collapses create localized hotspots with extreme temperatures and pressures (Ziarani et al., 2019), providing the necessary activation energy for C–O bond cleavage more efficiently than conventional heating (Fan et al., 2018). Thus, ultrasound acts as a powerful physical promoter that accelerates the nucleophilic attack without altering the fundamental chemical pathway. The differences between previous studies and the present study are summarized in the **Table 2**

The structure of compound a, b, and c are illustrated in **Figure 4** and The comparative FTIR spectra data of compound **a**, **b** and **c** are presented in **Figure 5.**

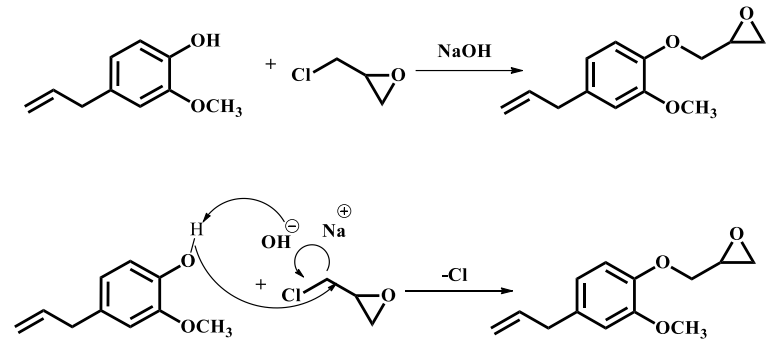

Figure 2. Reaction mechanism for the formation of the epoxide-substituted precursor compound

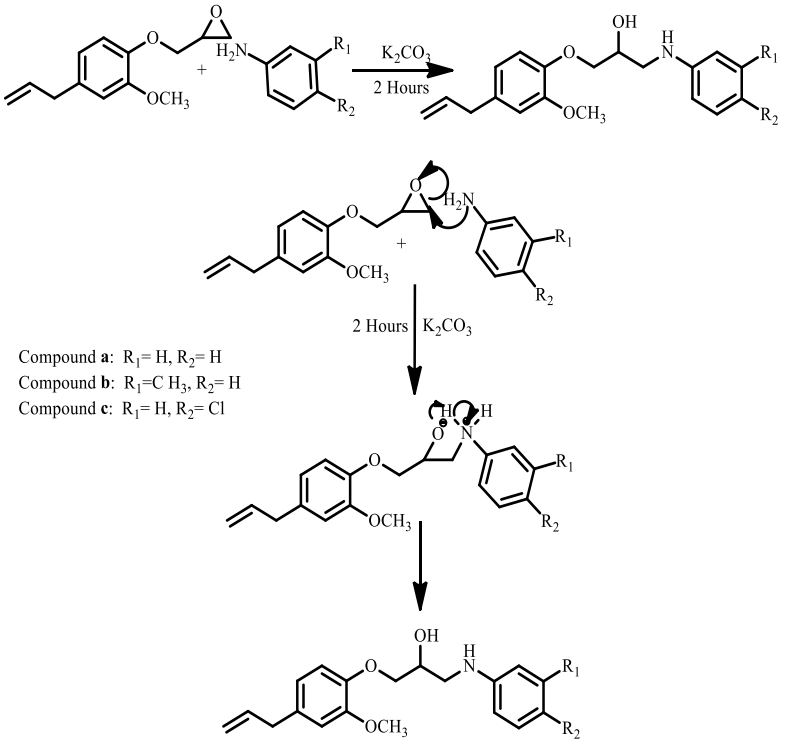

Figure 3. Mechanism for the synthesis of eugenol derivatives **a**, **b**, and **c**.

Table 2. Comparative analysis of synthesis parameters and effectiveness of eugenol derivatives

Reference	Methods	Result Compounds	Time	Yield
Bilgiçli et al. (2019)	Conventional Method	• *1-(4-Allyl-2-methoxyphenoxy)-3-(allylamino)propan-2-ol (95%)* • *1-(4-Allyl-2-methoxyphenoxy)-3-((cyclohex-1-en-1-ylmethyl) amino)propan-2-ol (78%)* • *1-(4-Allyl-2-methoxyphenoxy)-3-(tert-butylamino)propan-2-ol (98%)* • *1-(4-Allyl-2-methoxyphenoxy)-3-(diethylamino)propan-2-ol (80%)* • *1-(4-Allyl-2-methoxyphenoxy)-3-((pyridin-3-ylmethyl)amino) propan-2-ol (82%)*	5-24 hours	78-95%
Bilgiçli et al. (2020)	Conventional Method	• *propyl amine derivatives*	24 hours	58-81%
This Research	Ultrasonic Method	• *1-(4-allyl-2-methoxyphenoxy)-3-(phenylamino)propan-2-ol (91.66%)* • *1-(4-allyl-2-methoxyphenoxy)-3-(m-tolylamino)propan-2-ol (89.34%)* • *1-(4-allyl-2-methoxyphenoxy)-3-((4 chlorophenyl)amino)propan-2-ol (97.24%)*	2 hours	97.24 - 91.66%

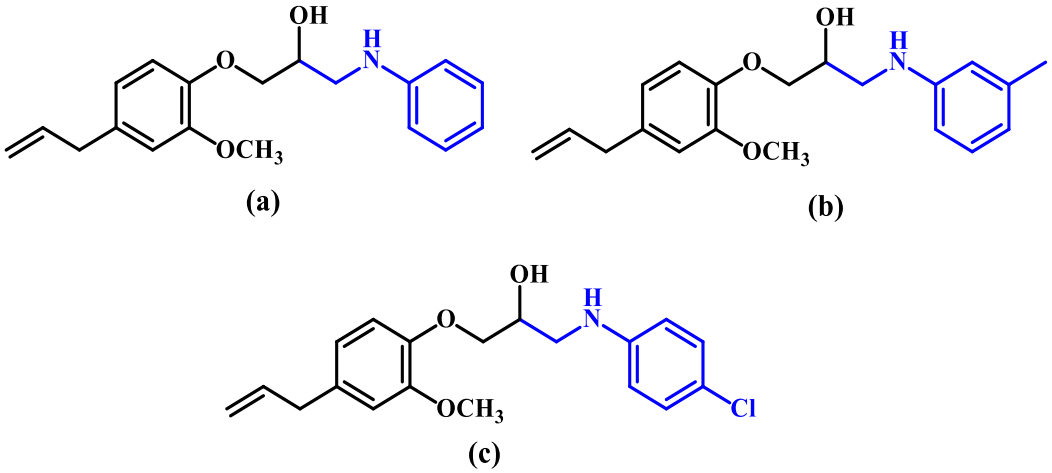

Figure 4. Structure eugenol derivatives **a**, **b**, and **c.**

Characterization

The evolution of the reaction was scrutinized using TLC analysis, confirming that the resulting chemical entities were purified and structurally confirmed by Melting point test, FTIR, NMR, and GC-MS analyses.

To confirm the formation of the precursor compound, several analysis and characterizations were performed. The formation of the precursor is indicated by a spot at an Rf value of 0.8, which is distinct from eugenol with an Rf of 0.725 using chloroform 100% as eluent. The synthesized precursor is an oily, golden-yellow substance with a yield of 70.48%. FT-IR characterization results show a spectral pattern identical to previous literature, evidenced by a peak at 1141 cm^{-1} representing the C-O ether group absorption and peaks within the 1270–1030 cm^{-1} range indicating C-O-C ether absorption. Furthermore, GC-MS analysis supports the formation of this compound with a retention time (Rt) of 34.5 minutes, an abundance of 71.31%, and an m/z of 220, which corresponds to the molecular weight of the precursor with the chemical formula $C_{13}H_{16}O_3$.

(1-(4-allyl-2-methoxyphenoxy) -3- (phenylamino) propan-2-ol) (**a**): oily yellow, Rf ($CHCl_3$ 100%): 0.20; Yield (91.66%), FT-IR spectra (cm^{-1}) 3487 (O-H), 3395 (N-H), 3055 (C-H sp2), 1604 and 1512 (C=C), 2931 (C-H sp3), 1257 (C-N), 1141 (C-O-C ether); ^{1}H-NMR 500 MHz, $CDCl_3$ (δ in Hz, type): 3.59, m, C-OH, 4.03, d (8.5), CH_2-O, 6.76, s, H-Ar, 6.78, d (7.5), H-Ar, 6.74, d (7.5), H-Ar, 3.85, s, O-CH_3, 3.82, dd (6.5 & 11.7), HC-Ar, 5.99, m, =CH, 5.10, d (8.5), H_2C=, 3.36, dd (6.5 & 5.2), CH_2-N, 6.65, d (8.5), H-Ar, 7.21, t (8.5), H-Ar, 6.86, d (4.0), H-Ar, 6.65, d (8.5), H-Ar, 7.21, t (8.5), H-Ar, 4.25, s, OH, 4.00, s, NH. ^{13}C-NMR, 125 MHz, $CDCl_3$: 68.54, C-OH, 72.58, O-CH_2, 148.24, O-CAr , 149.34, O-CAr, 114.45, CAr, 133.86, CAr, 120.79, CAr, 112.33, CAr, 55.73, O-CH_3, 39.78, CH_2, 137.68, =CH, 115.95, =CH_2,

46.51, CH_2-N, 146.28, CAr-N, 113.23, Ar-C, 129.21, Ar-C, 113.23, Ar-C, 129.21, Ar-C; MS m/z): 313 $[M]^+$, 164, 149, 132, 115, 106, 91, 77, 65, 51, 39, 28.

(1-(4-allyl-2-methoxyphenoxy)-3- (m-tolylamino) propan-2-ol) (b): Oily yellow, Rf ($CHCl_3$ 100%): 0.22; Yield (89.34%), FT-IR Spectra: (cm^{-1}) 3487 (O-H), 3395 (N-H), 3047 (C-H sp2), 1604 and 1512 (C=C), 2916 (C-H sp3), 1265 (C-N), 1141 (C-O-C ether); 1H-NMR 500 MHz, $CDCl_3$ (δ in Hz, type): 3.59, m, C-OH, 4.10, d (6.4), 6.74, s, H-Ar, 6.84, d (8.0), H-Ar, 5.05, t (8.5), H-Ar, 3.86, s, O-CH_3, 3.25, dd (6.8), HC-Ar, 5.96, m, =CH, 5.05, t (8.5), H_2C=, 3.34, dd (6.4), CH_2-N, 6.55, t (8.5), H-Ar, 6.49, d (7.7), H-Ar, 7.07, t (7.3), H-Ar, 6.47, d (7.3), H-Ar, 2.28, s, H-Ar, 4.23, s, OH, 4.00, s, NH; ^{13}C-NMR, 125 MHz, $CDCl_3$: 68.63, C-OH, 73.06, CH_2-O, 148.32, O-CAr, 149.66, O-CAr, 115.06, CAr, 134.19, CAr, 120.83, CAr, 112.37, CAr, 55.87, O-CH3, 39.85, CH_2, 137.53, =CH, 115.82, =CH_2, 46.64, CH_2-N, 146.43, CAr-N, 114.04, CAr, 139.09, CAr, 118.83, CAr, 129.18, CAr , 110.60, CAr, 21.70, Ar-C; MS data (m/z): 328 [M]+, 310, 298, 279, 236, 203, 161, 147, 120, 91

(1-(4-allyl-2-methoxyphenoxy)-3-((4 chlorophenyl) amino)propan-2-ol) (c): yellow solid; Rf ($CHCl_3$ 100%): 0.34; MP: 72 ℃; Yield (97.24%). FT- IR spectra (cm^{-1}) 3441 (O-H), 3387 (N-H), 3070 (C-H sp2), 1597 and 1512 (C=C), 2916 (C-H sp3), 1257 (C-N), 1141 (C-O-C ether), 818 (C-Cl); 1H-NMR 500 MHz, $CDCl_3$ (δ in Hz, type): 3.59, s, HC-O, 4.10, d (3.6), H_2C-O, 6.72, s, H-Ar, 6.71, d (1.9), H-Ar, 6.86, d (1.9), H-Ar, 3.85, s, O-CH3, 3.22, dd (7.0), HC-Ar, 5.96, m, =CH, 5.05, dd (7.3), =CH_2, 3.34, d (7.0), CH_2-N, 6.54, d (8.6), H-Ar, 7.10, d (8.6), H-Ar, 7.10, d, (8.6), H-Ar, 6.54, d (8.6), H-Ar, 4.21, s, OH, 4.00, s, NH; ^{13}C-NMR, 125 MHz, $CDCl_3$: 68.61, C-OH, 73.39, CH_2-O, 146.98, O-CAr, 149.96, O-CAr, 114.37, CAr, 134.70, CAr, 120.91, CAr, 112.48, CAr, 55.89, O-CH_3, 39.95, CH_2, 137.51, =CH, 115.95, =CH_2, 46.67, CH_2-N, 146.33, CAr-N, 115.78, CAr, 129.15, CAr, 115.78, CAr, 129.15, CAr; MS data (m/z): 347 $[M]^+$, 183, 164, 140, 130, 104, 77, 41.

Fragmentation analysis obtained from mass spectrometry was also performed to confirm that the observed fragments correspond to those of the target structures (Yamamoto et al., 2024; Nikolskiy et al., 2015) for compounds **a**, **b**, and **c**, as illustrated in **Figure 6.** These findings highlight the potential of sonochemical synthesis as a green and time-efficient approach for preparing eugenol-based derivatives.

Preliminary Enzyme–Ligand Interaction Study (In Vitro Assay)

Based on the tested concentration range (62.5–1000 μM), all compounds (**a**, **b**, **c**) and acarbose exhibited more than 90% inhibition at the lowest concentration tested. Therefore, their IC_{50} values are estimated to be lower than 62.5 μM and could not be accurately determined within the current experimental range. % Inhibition Data could be seen in **Table 3.**

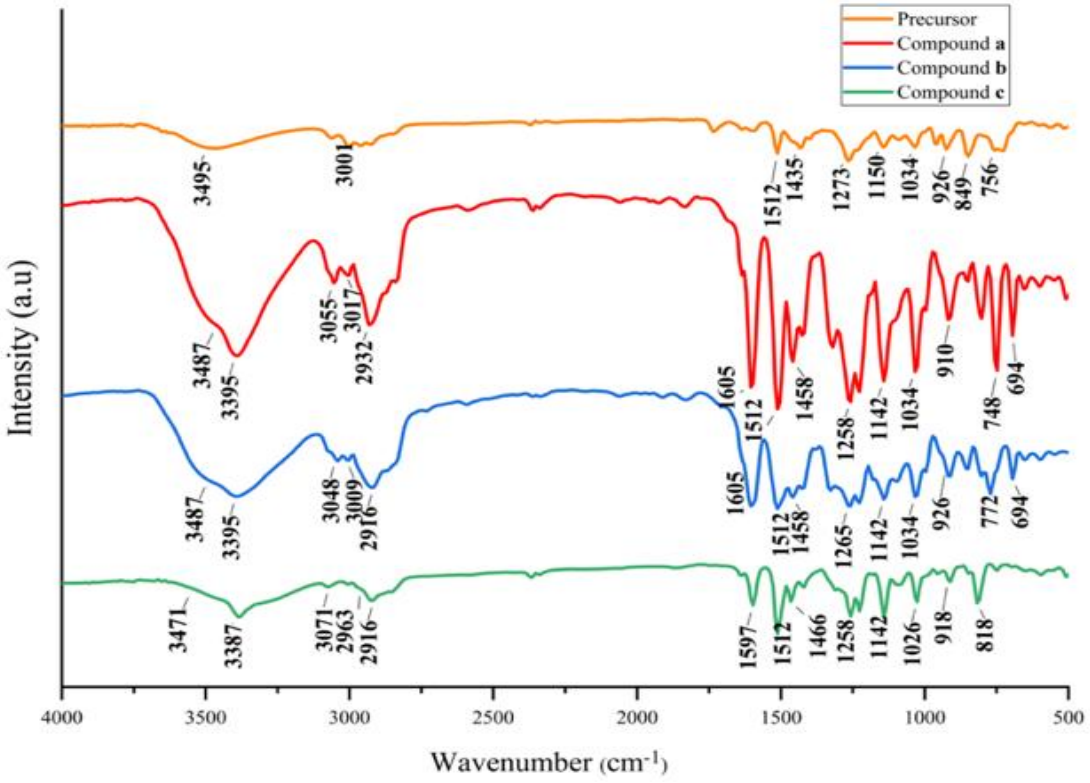

Figure 5. FTIR spectra of eugenol substituted epoxide, compound **a**, **b** and **c**

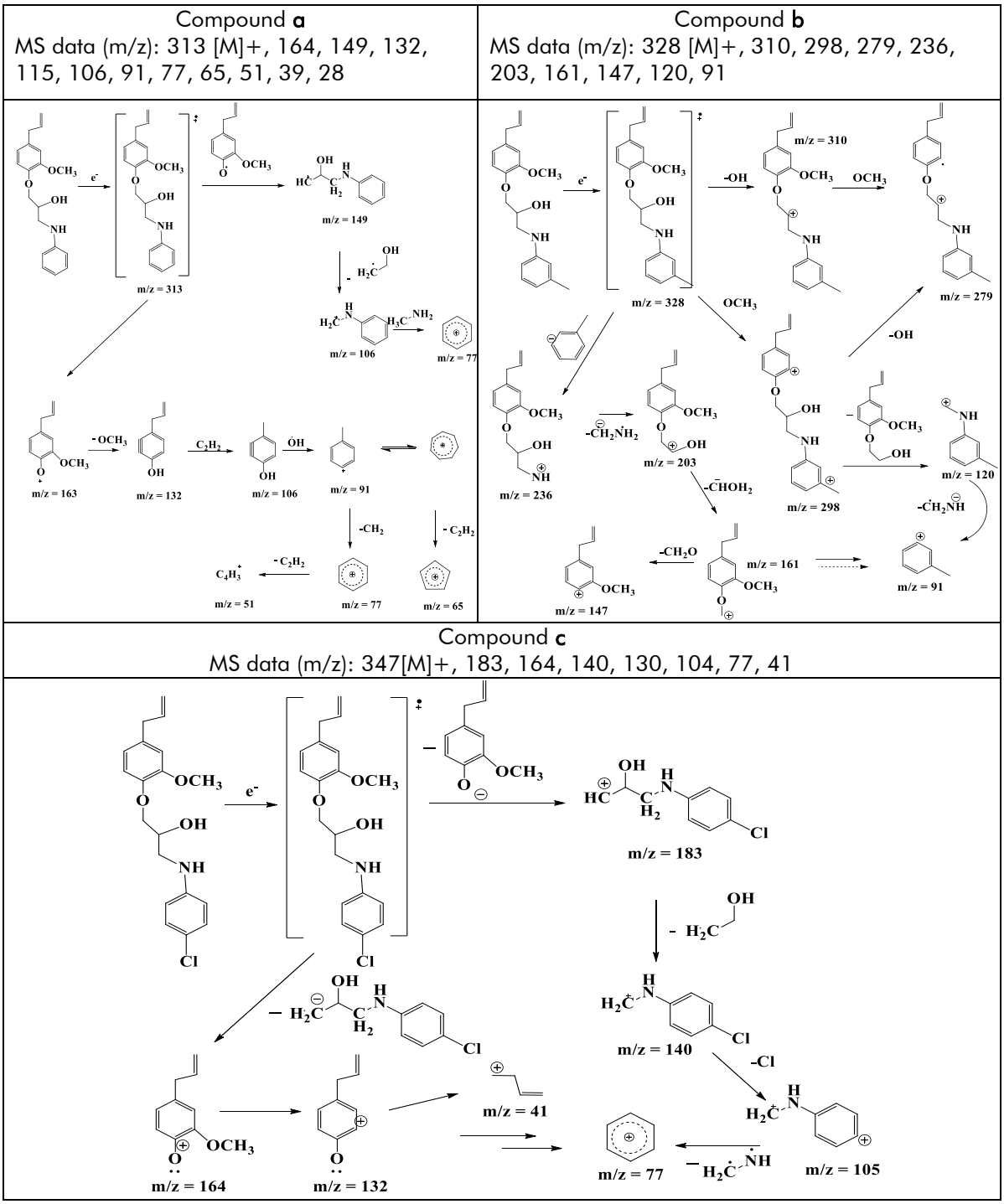

Figure 6. Fragmentation of compound **a**, **b**, and **c**

Table 3. Inhibition enzyme activities of compound **a, b,** and **c**

Conc. (μM)	Inhibitory Activity (%)			
	a	b	c	Acarbose
1000	98.86	99.57	99.51	98.85
500	98.82	99.20	99.20	98.77
250	98.80	99.04	98.82	97.99
125	93.80	97.49	97.47	97.03
62.5	93.49	97.10	96.92	95.92

Compound **a**, containing an unsubstituted phenyl ring, displayed baseline inhibitory activity. The introduction of a methyl substituent (-CH_3) in derivative **b** facilitated an enrichment of the aromatic phi-system through its electron-releasing properties, thereby enhancing hydrogen bonding and overall inhibition efficiency. Conversely, the electron-withdrawing chloro group (–Cl) in compound **c** reduced electron density and consequently weakened the interaction with α-amylase. These substituent effects are consistent with established structure–activity relationships, where activating groups enhance enzyme binding while deactivating groups reduce it (Guan et al., 2022; Saddique et al., 2022). No previous studies have specifically examined the influence of H, –CH_3, and –Cl substituents in eugenol-based aminopropoxy systems; thus, this study provides new structural insight into how substituent polarity modulates α-amylase binding affinity (Sołtysiak et al., 2020; Tobajas-Curiel et al., 2023).

Molecular Interaction Analysis (In Silico Docking Study)

To authenticate the reliability of the docking parameters, we initiated a self-docking exercise by repositioning the standard ligand at the α-amylase active site. The resulting RMSD value of 0.72 Å, well below the accepted threshold of 2 Å, confirmed that the docking parameters reliably reproduced the crystallographic binding orientation. Molecular Docking result is shown in **Table 4**.

When compared with reported α-amylase inhibitors such as thiohydantoin (–4.4 to –9.6 kcal mol^{-1}), chromone (–6.9 to –10.16 kcal mol^{-1}), and xanthene derivatives (–5.43 to –6.25 kcal mol^{-1}), the calculated binding energies were moderate but structurally consistent (Mezoughi et al., 2021; Sujatha, 2025). These findings suggest that while the compounds exhibit favorable binding interactions, further structural optimization may enhance their interaction strength (Sharma et al., 2025). The 2D docking interaction diagrams of the three ligands within the α-amylase active site are shown in **Figure 7**.

Compound **a** primarily formed van der Waals, hydrogen bonding, π–anion, π–π stacking, π–π T-shaped, and alkyl/π–alkyl interactions. Compound **b** showed a simpler interaction profile mainly van der Waals, hydrogen bonding, π–σ, π–π stacking, alkyl, and π–alkyl contacts yet retained a comparable binding affinity to compound **c**, which exhibited slightly more interaction types including carbon–hydrogen, π–anion, and π–π T-shaped bonding. All three derivatives displayed stronger affinities than acarbose (–3.64 kcal mol^{-1}), which interacted mainly through van der Waals and conventional hydrogen bonds.

Table 4. Molecular Docking result

Ligand Name	ΔG (kcal/mol)	Ki (mM)
Acarbose	-3.64	2.150
Compound **a**	-4.58	0.437
Compound **b**	-5.13	0.174
Compound **c**	-5.16	0.164

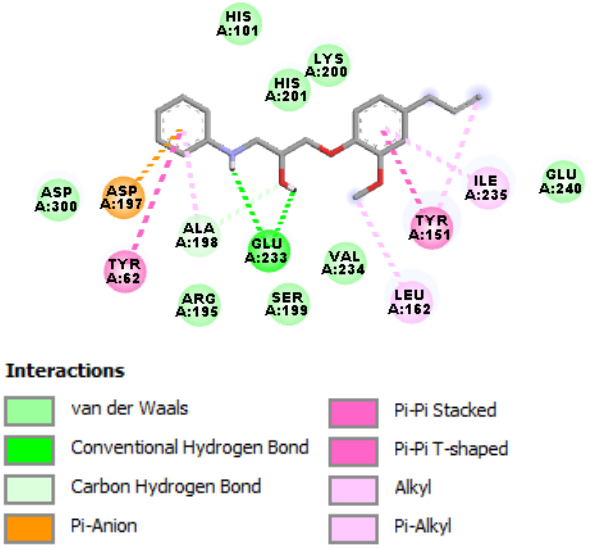

Compound **a**

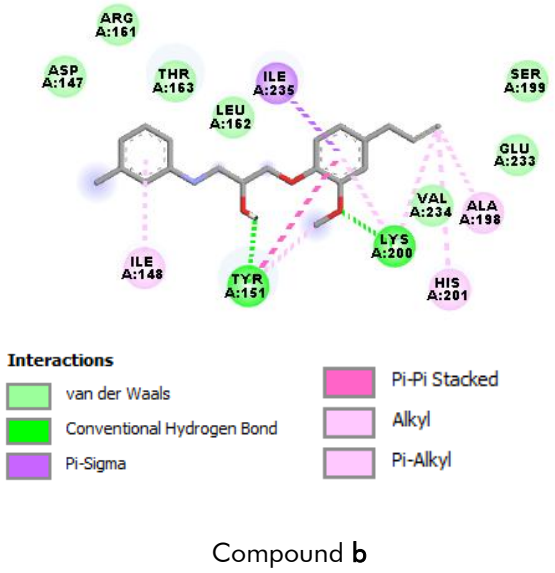

Compound **b**

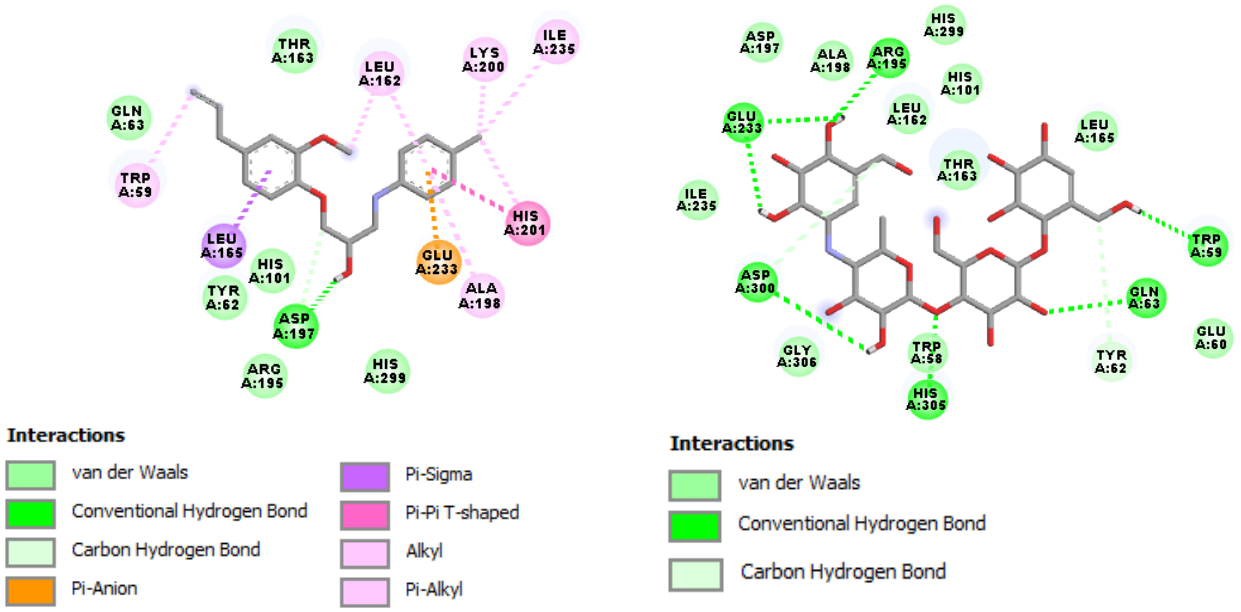

Compound **c** Acarbose

Figure 7. Interactions between compound **a**, **b**, **c** and acarbose with enzyme α-amylase

Variations in the binding interactions are attributed to substituent-driven electronic effects on the aromatic ring. The methyl substituent in compound **b** donates electron density, reinforcing *π–π* and hydrogen-bond interactions, whereas the chlorine atom in compound **c** withdraws electrons, slightly weakening its interaction energy. Such substituent effects directly influence both the electron distribution and binding affinity of the molecule. Previous reports have emphasized that substituent type and spatial position critically modulate α-amylase binding efficiency (Visvanathan et al., 2024; Khan et al., 2022). Hydrogen bonding served as the main stabilizing force, with hydrophobic and *π*–alkyl interactions contributing secondarily an interaction pattern consistent with other aromatic derivatives such as benzopyran, thiazole, and indole compounds (Zong et al., 2023; Kuczyńska et al., 2023; Sharma et al., 2020). These results confirm that the electronic nature and position of substituents profoundly affect the molecular interaction pattern and binding strength of aminated eugenol derivatives with the α-amylase active site.

CONCLUSIONS

Three aminated eugenol derivatives (**a**, **b**, and **c**) were successfully synthesized through an ultrasound-assisted method that efficiently reduced the reaction time to 2 hours while affording high yields of up to 97.24%. Comprehensive spectroscopic characterization (FTIR, NMR, and GC-MS) confirmed the formation of aminopropoxy linkages through nucleophilic epoxide ring-opening. Preliminary enzyme–ligand interaction analysis indicated that all derivatives interact more strongly with α-amylase than the reference compound acarbose, with compound b showing the best inhibition properties (99.04% at 250 *μM*) and supported by its molecular docking result (binding affinity value –5.13 kcal mol) which highlights the strong potential of these eugenol derivatives as antidiabetic drug candidates.

A ACKNOWLEDGEMENTS

The authors extend their appreciation to Lembaga Penelitian dan Pengabdian kepada Masyarakat Universitas Hasanuddin for funding this research with grant number: 01260/UN4.22/PT.01.03/2025.

Conflict of Interest The authors declare no conflict of interest.

REFERENCES

Ahmed, D., Khan, M., & Saeed, R. (2023). Inhibition kinetics of α-amylase by plant polyphenols using UV–Vis spectroscopy: A potential approach for diabetes management. *Food Chemistry, 402,* 134088. https://doi.org/10.1016/j.foodchem.2022.134088

Bilgiçli, H. G., Ergon, D., Taslimi, P., Tuzun, B., Kuru, I. A., Zengin, M., & Gülçin, İ. (2020). Novel propanolamine derivatives attached to 2-methoxyphenol moiety: Synthesis, characterization, biological properties, and molecular docking studies. *Bioorganic Chemistry, 101,* 103969. https://doi.org/10.1016/j.bioorg.2020.103969

Bilgiçli, H. G., Kestane, A., Taslimi, P., Karabay, O., & Bytyqi-Damoni, A. (2019). Novel eugenol bearing oxypropanolamines: Synthesis, characterization, antibacterial, antidiabetic, and anticholinergic potentials. *Bioorganic Chemistry, 88,* 1–7. https://doi.org/10.1016/j.bioorg.2019.102931

Cerna, M. (2020). Epigenetic regulation in etiology of type 1 diabetes mellitus. *International Journal of Molecular Sciences, 21*(1), 36. https://doi.org/10.3390/ijms21010036

Chaudhari, Y. S., Matkar, S. S., Bhujbal, S. S., Walunj, V. A., Bhor, N. S., & Vyavhare, R. D. (2023). Diabetes mellitus: A review. *International Journal of Advanced Research in Science Communication and Technology (IJARSCT), 3*(1), 5–9. https://doi.org/10.48175/ijarsct-8551

Ekbrant, B. E. F., Skov, A. L., & Daugaard, A. E. (2021). Epoxy-rich systems with preference for etherification over amine-epoxy reactions for tertiary amine accelerators. *Macromolecules, 54*(9), 4280–4287. https://doi.org/10.1021/acs.macromol.0c02630

Fan, Y., Cheng, C., Li, J., Yuan, Q., Wang, X., & Liu, X. (2018). The discovery of ultrasound irradiation as a useful tool for accelerating Petasis three-component reaction: Synthesis of α-arylglycines. *Ultrasonics Sonochemistry, 46,* 52–58. https://doi.org/10.1016/j.ultsonch.2018.04.013

Fatiha, M., Fatma, B., Awatif, B., Nesrine, A., & Noureddine, D. (2018). Antidiabetic bioactive compounds from plants. *Journal of Medical Technology, 2*(2), 199–214. https://doi.org/10.26415/2572-004X-vol2iss1 p199-24

Guan, L., Long, H., Ren, F., Li, Y., & Zhang, H. (2022). A structure–activity relationship study of the inhibition of α-amylase by benzoic acid and its derivatives. *Nutrients, 14*(9), 1931. https://doi.org/10.3390/nu14091931

Julianto, T. S., Rachmawaty, F. J., Tamhid, H. A., & Putri, B. S. (2023). The potential antimalarial drug of aryl amino alcohol derivatives from eugenol: Synthesis, in-vitro and in-silico analysis of bioactivity. *Rasayan Journal of Chemistry, 16*(3), 1425–1434. https://doi.org/10.31788/rjc.2023.1636940

Kaufman, T. S. (2015). The multiple faces of eugenol: A versatile starting material and building block for organic and bio-organic synthesis and a convenient precursor toward bio-based fine chemicals. *Journal of the Brazilian Chemical Society, 26*(6), 1055–1085. https://doi.org/10.5935/0103-5053.20150086

Khan, M., Ullah, S., Rahim, F., Taha, M., Hussain, R., Khan, M. S., Ali, H., Khan, M. U., Shah, S. A. A., Khan, K. M. (2022). New thiazole-based thiazolidinone derivatives: Synthesis, *in vitro* α-amylase, α-glucosidase activities and *in silico* molecular docking study. *Chemical Data Collections, 42*, 100967. https://doi.org/10.1016/j.cdc.2022.100967

Kuczyńska, A., Szkudlarek, A., Ratajczak-Sitarz, M., Glensk, M., & Kaczmarek, M. (2023). Structural and biochemical characterization of α-amylase inhibitors for potential antidiabetic drug discovery. *International Journal of Molecular Sciences, 24*(14), 11820. https://doi.org/10.3390/ijms241411820

Ling, H., Yu, X., Wang, S., Wang, X., & Dong, L. (2018). Study on ultrasonic assisted mechanism of ring opening polymerization of octamethylcyclotetrasiloxane (D4). *AIP Conference Proceedings, 1971*(1), 020003. https://doi.org/10.1063/1.5041098

Mezoughi, A. B., Abdussalam-Mohammed, W., & Abdusalam, A. (2021). Synthesis and molecular docking studies of some thiohydantoin derivatives as potential anticancer and antimicrobial agents. *Advances in Journal of Chemistry A, 4*(6), 317–326. https://doi.org/10.22034/AJCA.2021.291823.1266

Mnafgui, K., Kaanich, F., Derbali, A., Hamden, K., Derbali, F., Slama, S., Allouche, N., & Elfeki, A. (2013). Inhibition of key enzymes related to diabetes and hypertension by eugenol in vitro and in alloxan-induced diabetic rats. *Archives of Physiology and Biochemistry,* 1–9. https://doi.org/10.3109/13813455.2013.822521

Molina-Gutiérrez, S., Manseri, A., Ladmiral, V., Bongiovanni, R., & Caillol, S. (2019). Eugenol: A promising building block for synthesis of radically polymerizable monomers. *Macromolecular Chemistry and Physics, 220*(14), 1900179. https://doi.org/10.1002/MACP.201900179

Nampoothiri, S. V., Prathapan, A., Cherian, O. L., Raghu, K. G., Venugopalan, V. V., & Sundaresan, A. (2011). In vitro antioxidant and inhibitory potential of *Terminalia bellerica* and *Emblica officinalis* fruits against LDL oxidation and key enzymes linked to type 2 diabetes. *Food and Chemical Toxicology, 49,* 125–131. https://doi.org/10.1016/j.fct.2010.10.006

Nasef, M. M., Zakeri, M., Asadi, J., Abouzari-Lotf, E., Ahmad, A., & Malakooti, R. (2016). Environmentally benign and highly regioselective ring opening of epoxides accelerated by ultrasound irradiation. *Green Chemistry Letters and Reviews, 9*(1), 76–84. https://doi.org/10.1080/17518253.2015.1137975

Nikolskiy, I., Siuzdak, G., & Patti, G. J. (2015). Discriminating precursors of common fragments for large-scale metabolite profiling by triple quadrupole mass spectrometry. *Bioinformatics, 31*(12), 2017–2023. https://doi.org/10.1093/bioinformatics/btv085

Patel, J., Singh, H., & Kumar, R. (2023). Computational approaches in drug discovery: Advances in molecular docking and virtual screening. *Drug Design, Development and*

Therapy, 17(1), 987–1005. https://doi.org/10.2147/DDDT.S392874

Rafique, R., Khalid, M., Arshia, A., Kanwal, A., Sridevi, C., Abdul, W., Ashfaq, R., Arunkumar, K., Shehryar, H., & Al-Rashida, M. (2020). Synthesis of new indazole-based dual inhibitors of α-glucosidase and α-amylase enzymes: Their in vitro, in silico, and kinetics studies. *Bioorganic Chemistry, 94,* 103195. https://doi.org/10.1016/j.bioorg.2019.103195

Roy, S., Pokharel, P., & Piganelli, J. D. (2024). Decoding the immune dance: Unraveling the interplay between beta cells and type 1 diabetes. *Molecular Metabolism, 88,* 101998. https://doi.org/10.1016/j.molmet.2024.101998

Saddique, F. A., Ahmad, M., Ashfaq, U. A., Muddassar, M., Sultan, S., & Zaki, M. E. A. (2022). Identification of cyclic sulfonamides with an N-arylacetamide group as α-glucosidase and α-amylase inhibitors: Biological evaluation and molecular modeling. *Pharmaceuticals (Basel), 15*(1), 106. https://doi.org/10.3390/ph15010106

Saputri, E., Karisma, F., Fakhmi, N., Kusumaningtyas, E., Priyatama, D., & Santoso, B. (2016). Docking molekular potensi anti-diabetes melitus tipe 2 turunan zerumbon sebagai inhibitor aldosa reduktase dengan Autodock-Vina. *Chimica et Natura Acta, 4*(1), 16–20. https://doi.org/10.24198/cna.v4.n1.10443

Shabalala, N. G., Kerru, N., Maddila, S., van Zyl, W. E., Jonnalagadda, S. B. (2020). Catalyst-free synthesis of novel isopropyl 2-amino-7,7-dimethyl-4-aryl-5-oxo-5,6,7,8-tetrahydro-4H-chromene-3-carboxylate derivatives in aqueous ethanol under ultrasound irradiation. *Chemical Data Collections, 28,* 100365. https://doi.org/10.1016/j.cdc.2020.100365

Sharma, R., Rani, R., Gupta, A., & Singh, J. (2020). Design, synthesis, and biological evaluation of substituted eugenol derivatives as α-amylase inhibitors with potential antidiabetic activity. *Journal of Medicinal Chemistry, 63*(1), 146–159. https://doi.org/10.1021/acs.jmedchem.9b01611

Sharma, R., Shilpa, & Duggal, S. (2025). Exploring binding affinities and interactions of benzimidazole derivatives via AutoDock molecular docking studies. *Asian Journal of Research in Chemistry, 18*(3), 123–128. https://doi.org/ 10.52711/0974-4150.2025.00020

Sołtysiak, P., Dziuk, B., Zarychta, B., Ejsmont, K., & Spaleniak, G. (2020). The substituent effect of π-electron delocalization in N-methylamino-nitropyridine derivatives: Crystal structure and DFT calculations. *Structural Chemistry, 31,* 1185–1196. https://doi.org/10.1007/s11224-020-01514-y

Sujatha, G. (2025). Synthesis and docking studies of some novel heterocyclic moieties acting as superior inhibitors. *Research Journal of Chemistry and Environment, 28*(8), 16–22. https://doi.org/10.25303/288rjce016022

Thirumalaikumar, M. (2022). Ring opening reactions of epoxides: A review. *Organic Preparations and Procedures International, 54*(1), 1–39. https://doi.org/10.1080/10406638.2023.2235055

Tobajas-Curiel, G., Sun, Q., Sanders, J. K., Ballester, P., & Hunter, C. A. (2023). Substituent effects on aromatic interactions in water. *Chemical Science.* https://doi.org/10.1039/d3sc01027a

Visvanathan, R., Houghton, M. J., & Williamson, G. (2024). Structure–function relationships in (poly)phenol–enzyme binding: Direct inhibition of human salivary and pancreatic α-amylases. *Food Research International, 188*, 114504. https://doi.org/10.1016/j.foodres.2024.114504

Wang, J., Liu, X., Shen, C., & Zhang, W. (2024). Advances in molecular docking for drug discovery: Methods, applications, and challenges. *Journal of Medicinal Chemistry, 67*(2), 1123–1145. https://doi.org/10.1021/acs.jmedchem.3c01456

Yamamoto, A., Tokai, N., Kakehashi, R., & Saigusa, D. (2024). Fragmentation considerations using amidoamine oxide homologs. *Mass Spectrometry (Tokyo), 13*(1), A0158. https://doi.org/10.5702/massspectrometry.A0158

Ziarani, G.M., Kheilkordi, Z., & Gholamzadeh, P. (2019). Ultrasound-assisted synthesis of heterocyclic compounds. *Molecular Diversity, 24*(8), 771–820. https://doi.org/10.1007/s11030-019-09964-1

Zong, X., Jiang, W., Lu, M., Wang, Y., & Liu, H. (2023). Insights into the molecular structure, conformation and electronic properties of drug molecules through advanced computational chemistry. *Coordination Chemistry Reviews, 496*, 215385. https://doi.org/10.1016/j.ccr.2023.215385